

AG



SCAN-9409192

SW 3430

ICHEP94 Ref. GLS0253
Submitted to PA 21,2 Pl 9,19

CLEO CONF 94-19
July 19, 1994

Form Factor Ratio Measurement in $\Lambda_c^+ \rightarrow \Lambda e^+ \nu_e$

J. Dominick,¹ M. Lambrecht,¹ S. Sanghera,¹ V. Shelkov,¹ T. Skwarnicki,¹ R. Stroynowski,¹
I. Volobouev,¹ G. Wei,¹ P. Zadorozhny,¹ M. Artuso,² M. Gao,² M. Goldberg,² D. He,²
N. Horwitz,² G.C. Moneti,² R. Mountain,² F. Muheim,² Y. Mukhin,² S. Playfer,²
Y. Rozen,² S. Stone,² X. Xing,² G. Zhu,² J. Bartelt,³ S.E. Csorna,³ Z. Egyed,³ V. Jain,³
D. Gibaut,⁴ K. Kinoshita,⁴ P. Pomianowski,⁴ B. Barish,⁵ M. Chadha,⁵ S. Chan,⁵
D.F. Cowen,⁵ G. Eigen,⁵ J.S. Miller,⁵ C. O'Grady,⁵ J. Urheim,⁵ A.J. Weinstein,⁵
M. Athanas,⁶ W. Brower,⁶ G. Masek,⁶ H.P. Paar,⁶ J. Gronberg,⁷ R. Kutschke,⁷
S. Menary,⁷ R.J. Morrison,⁷ S. Nakanishi,⁷ H.N. Nelson,⁷ T.K. Nelson,⁷ C. Qiao,⁷
J.D. Richman,⁷ A. Ryd,⁷ D. Sperka,⁷ H. Tajima,⁷ M.S. Witherell,⁷ R. Balest,⁸ K. Cho,⁸
W.T. Ford,⁸ D.R. Johnson,⁸ K. Lingel,⁸ M. Lohner,⁸ P. Rankin,⁸ J.G. Smith,⁸
J.P. Alexander,⁹ C. Bebek,⁹ K. Berkelman,⁹ K. Bloom,⁹ T.E. Browder,^{9*} D.G. Cassel,⁹
H.A. Cho,⁹ M.M. Coffman,⁹ D.S. Crowcroft,⁹ P.S. Drell,⁹ D. Dumas,⁹ R. Ehrlich,⁹
P. Gaidarev,⁹ D. Garcia-Sciveres,⁹ B. Geiser,⁹ B. Gittelman,⁹ S.W. Gray,⁹ D.L. Hartill,⁹
B.K. Heltsley,⁹ S. Henderson,⁹ C.D. Jones,⁹ S.L. Jones,⁹ J. Kandaswamy,⁹ N. Katayama,⁹
P.C. Kim,⁹ D.L. Kreinick,⁹ G.S. Ludwig,⁹ J. Masui,⁹ J. Mevissen,⁹ N.B. Mistry,⁹ C.R. Ng,⁹
E. Nordberg,⁹ J.R. Patterson,⁹ D. Peterson,⁹ D. Riley,⁹ S. Salman,⁹ M. Sapper,⁹
F. Würthwein,⁹ P. Avery,¹⁰ A. Freyberger,¹⁰ J. Rodriguez,¹⁰ S. Yang,¹⁰ J. Yelton,¹⁰
D. Cinabro,¹¹ T. Liu,¹¹ M. Saulnier,¹¹ R. Wilson,¹¹ H. Yamamoto,¹¹ T. Bergfeld,¹²
B.I. Eisenstein,¹² G. Gollin,¹² B. Ong,¹² M. Palmer,¹² M. Selen,¹² J. J. Thaler,¹²
K.W. Edwards,¹³ M. Ogg,¹³ A. Bellerive,¹⁴ D.I. Britton,¹⁴ E.R.F. Hyatt,¹⁴
D.B. MacFarlane,¹⁴ P.M. Patel,¹⁴ B. Spaan,¹⁴ A.J. Sadoff,¹⁵ R. Ammar,¹⁶ P. Baringer,¹⁶
A. Bean,¹⁶ D. Besson,¹⁶ D. Coppage,¹⁶ N. Coptay,¹⁶ R. Davis,¹⁶ N. Hancock,¹⁶ M. Kelly,¹⁶
S. Kotov,¹⁶ I. Kravchenko,¹⁶ N. Kwak,¹⁶ H. Lam,¹⁶ Y. Kubota,¹⁷ M. Lattery,¹⁷
M. Momayezi,¹⁷ J.K. Nelson,¹⁷ S. Patton,¹⁷ R. Poling,¹⁷ V. Savinov,¹⁷ S. Schrenk,¹⁷
R. Wang,¹⁷ M.S. Alam,¹⁸ I.J. Kim,¹⁸ Z. Ling,¹⁸ A.H. Mahmood,¹⁸ J.J. O'Neill,¹⁸
H. Severini,¹⁸ C.R. Sun,¹⁸ F. Wappler,¹⁸ G. Crawford,¹⁹ C. M. Daubennier,¹⁹ R. Fulton,¹⁹
D. Fujino,¹⁹ K.K. Gan,¹⁹ K. Honscheid,¹⁹ H. Kagan,¹⁹ R. Kass,¹⁹ J. Lee,¹⁹ R. Malchow,¹⁹
M. Sung,¹⁹ C. White,¹⁹ M.M. Zoeller,¹⁹ F. Butler,²⁰ X. Fu,²⁰ B. Nemati,²⁰ W.R. Ross,²⁰
P. Skubic,²⁰ M. Wood,²⁰ M. Bishai,²¹ J. Fast,²¹ E. Gerndt,²¹ R.L. McIlwain,²¹ T. Miao,²¹
D.H. Miller,²¹ M. Modesitt,²¹ D. Payne,²¹ E.I. Shibata,²¹ I.P.J. Shipsey,²¹ P.N. Wang,²¹
M. Battle,²² J. Ernst,²² L. Gibbons,²² Y. Kwon,²² S. Roberts,²² E.H. Thorndike,²² and
C.H. Wang²²

(CLEO Collaboration)

- ¹Southern Methodist University, Dallas, Texas 75275
²Syracuse University, Syracuse, New York 13244
³Vanderbilt University, Nashville, Tennessee 37235
⁴Virginia Polytechnic Institute and State University, Blacksburg, Virginia, 24061
⁵California Institute of Technology, Pasadena, California 91125
⁶University of California, San Diego, La Jolla, California 92093
⁷University of California, Santa Barbara, California 93106
⁸University of Colorado, Boulder, Colorado 80309-0390
⁹Cornell University, Ithaca, New York 14853
¹⁰University of Florida, Gainesville, Florida 32611
¹¹Harvard University, Cambridge, Massachusetts 02138
¹²University of Illinois, Champaign-Urbana, Illinois, 61801
¹³Carleton University, Ottawa, Ontario K1S 5B6 and the Institute of Particle Physics, Canada
¹⁴McGill University, Montréal, Québec H3A 2T8 and the Institute of Particle Physics, Canada
¹⁵Ithaca College, Ithaca, New York 14850
¹⁶University of Kansas, Lawrence, Kansas 66045
¹⁷University of Minnesota, Minneapolis, Minnesota 55455
¹⁸State University of New York at Albany, Albany, New York 12222
¹⁹Ohio State University, Columbus, Ohio, 43210
²⁰University of Oklahoma, Norman, Oklahoma 73019
²¹Purdue University, West Lafayette, Indiana 47907
²²University of Rochester, Rochester, New York 14627

Abstract

Using the CLEO II detector at CESR angular distributions of the decay $\Lambda_c^+ \rightarrow \Lambda e^+ \nu_e$ have been studied. By performing a 3-dimensional maximum likelihood fit, the form factor ratio, $R = f_2/f_1$, is extracted and found to be $-0.33 \pm 0.16 \pm 0.15$.

*Permanent address: University of Hawaii at Manoa

Charm semileptonic decays allow a measurement of the form factors which parametrize the hadronic current because the Cabibbo-Kobayashi-Maskawa (CKM) matrix element V_{cs} is known from unitarity [1]. Heavy Quark Effective Theory (HQET) [2] and SU(3) relate the form factors in $c \rightarrow s\ell\nu$ to the form factors in $b \rightarrow u$ decay, thereby allowing the determination of CKM matrix elements involving the b quark. Although this scheme was originally conceived for mesons, for which data have been more readily available, within HQET, Λ -type baryons are more straightforward to treat than mesons as they consist of a heavy quark and a spin zero light diquark. This simplicity also allows for more reliable predictions concerning heavy quark to light quark transitions [3] [4] [5] than is the case for mesons. It has therefore been argued that HQET can be applied to $\Lambda_c^+ \rightarrow \Lambda\ell^+\nu_\ell$. A measurement of the form factors in $\Lambda_c^+ \rightarrow \Lambda\ell^+\nu_\ell$ tests this idea. Since in HQET these form factors are related to those governing $\Lambda_b \rightarrow \Lambda_c^+\ell^-\bar{\nu}_\ell$ and $\Lambda_b \rightarrow p\ell^-\bar{\nu}_\ell$, it also offers alternative strategies for measuring the CKM matrix elements V_{cb} and V_{ub} .

In the limit of negligible lepton mass, the semileptonic decay of a charmed baryon $1/2^+ \rightarrow 1/2^+$ is usually parametrized in terms of four form factors: two axial form factors F_1^A and F_2^A , and two vector form factors F_1^V and F_2^V . These form factors are functions of q^2 , the invariant mass squared of the virtual W . In the zero lepton mass approximation, the decay may be described in terms of helicity amplitudes $H_{\lambda_\Lambda\lambda_W} = H_{\lambda_\Lambda\lambda_W}^V + H_{\lambda_\Lambda\lambda_W}^A$, where λ_Λ and λ_W are the helicities of the Λ and W . The helicity amplitudes are related to the form factors by:

$$\begin{aligned}\sqrt{q^2}H_{\frac{1}{2}0}^V &= \sqrt{Q_-}[(M_{\Lambda_c} + M_\Lambda)F_1^V - q^2F_2^V] \\ H_{\frac{1}{2}1}^V &= \sqrt{2Q_-}[-F_1^V + (M_{\Lambda_c} + M_\Lambda)F_2^V] \\ \sqrt{q^2}H_{\frac{1}{2}0}^A &= \sqrt{Q_+}[(M_{\Lambda_c} - M_\Lambda)F_1^A + q^2F_2^A] \\ H_{\frac{1}{2}1}^A &= \sqrt{2Q_+}[-F_1^A - (M_{\Lambda_c} - M_\Lambda)F_2^A]\end{aligned}\quad (1)$$

where $Q_\pm = (M_{\Lambda_c} \pm M_\Lambda)^2 - q^2$. The remaining helicity amplitudes can be obtained with the help of the parity relations: $H_{-\lambda_\Lambda-\lambda_W}^{V(A)} = +(-)H_{\lambda_\Lambda\lambda_W}^{V(A)}$.

In terms of the helicity amplitudes the four fold decay distribution, Γ_S , can be written as [5]:

$$\begin{aligned}\Gamma_S &= \frac{d\Gamma}{dq^2 d\cos\Theta_W d\cos\Theta_\Lambda d\chi} = B(\Lambda \rightarrow p\pi) \frac{1}{2} \frac{G_F^2}{(2\pi)^4} |V_{cs}|^2 \frac{q^2 P}{24M_{\Lambda_c}^2} \\ &\times \left\{ \frac{3}{8} (1 - \cos\Theta_W)^2 |H_{\frac{1}{2}1}^V|^2 (1 + \alpha_\Lambda \cos\Theta_\Lambda) + \frac{3}{8} (1 + \cos\Theta_W)^2 |H_{-\frac{1}{2}-1}^V|^2 (1 - \alpha_\Lambda \cos\Theta_\Lambda) \right. \\ &\quad \left. + \frac{3}{4} \sin^2\Theta_W [|H_{\frac{1}{2}0}^V|^2 (1 + \alpha_\Lambda \cos\Theta_\Lambda) + |H_{-\frac{1}{2}0}^V|^2 (1 - \alpha_\Lambda \cos\Theta_\Lambda)] \right. \\ &\quad \left. + \frac{3}{2\sqrt{2}} \cos\chi \sin\Theta_W \sin\Theta_\Lambda [(1 - \cos\Theta_W) \text{Re}(H_{-\frac{1}{2}0}^V H_{\frac{1}{2}1}^{*V}) + (1 + \cos\Theta_W) \text{Re}(H_{\frac{1}{2}0}^V H_{-\frac{1}{2}-1}^{*V})] \right\}\end{aligned}\quad (2)$$

where G_F is the Fermi coupling constant, V_{cs} is the CKM matrix element, P is the Λ momentum in the Λ_c rest frame, Θ_Λ is the angle between the momentum vector of the proton in the Λ rest frame and the Λ momentum in the Λ_c rest frame, Θ_W is the angle between the momentum vector of the electron in the W rest frame and the Λ momentum in

the Λ_c rest frame, χ is the angle between the Λ and W decay planes in the Λ_c rest frame, and α_Λ is the $\Lambda \rightarrow p\pi$ decay asymmetry parameter measured to be 0.64 [1].

Within the framework of HQET the heavy flavor and spin symmetries imply relations among the form factors which reduce their number to one when the decay involves only heavy quarks [3] [6]. Treating the s quark as a light quark, two independent form factors f_1 and f_2 to $O(\bar{\Lambda}/m_s)$ [3] [4] are required to describe the hadronic current. The relationship between these form factors and the standard form factors is:

$$\begin{aligned}F_1^V(q^2) &= -F_1^A(q^2) = f_1(q^2) + \frac{M_\Lambda}{M_{\Lambda_c}} f_2(q^2) \\ F_2^V(q^2) &= -F_2^A(q^2) = \frac{1}{M_{\Lambda_c}} f_2(q^2)\end{aligned}\quad (3)$$

In general f_2 is expected to be less than f_1 . If the strange quark is treated as heavy f_2 is zero.

In order to extract the form factor ratio $R = f_2/f_1$ from a fit to Γ_S an assumption must be made about the q^2 dependence of the form factors. We follow the model of Körner and Krämer (KK) [5] who use the dipole form:

$$f(q^2) = \frac{f(q_{max}^2)}{(1 - q^2/m_{ff}^2)^2 (1 - q_{max}^2/m_{ff}^2)^2}\quad (4)$$

where the pole mass is chosen to be $m_{ff} = 2.11\text{GeV}/c^2$.

The data sample used in this study was collected with the CLEO II detector [7] at the Cornell Electron Storage Ring (CESR). The integrated luminosity consists of 3.0fb^{-1} taken at and just below the $\Upsilon(4S)$ resonance, which corresponds to approximately 4 million $e^+e^- \rightarrow c\bar{c}$ events.

We search for the decay $\Lambda_c^+ \rightarrow \Lambda e^+\nu_e$ in $e^+e^- \rightarrow c\bar{c}$ events by detecting a Λe^+ pair with invariant mass in the range $m_\Lambda < m_{\Lambda e^+} < m_{\Lambda_c}$ [8]. The minimum allowed momentum for electrons is $0.7\text{GeV}/c$. The Λ is reconstructed through its decay to $p\pi$. The dE/dx measurement of the proton is required to be consistent with the expected value. We require the momentum of the $p\pi$ pair to be greater than $0.8\text{GeV}/c$ in order to reduce background. These Λ candidates are then combined with electrons, and the sum of Λ and e^+ momentum, $p_{\Lambda e^+}$, is required to be greater than $1.4\text{GeV}/c$. This cut reduces our dependence on the shape of the Λ_c fragmentation function at low momentum, which is poorly known.

The number of events passing the cuts described above is 1101, of which 135_{-14}^{+22} are consistent with fake Λ background, 133 ± 40 are consistent with fake electron background and 116 ± 23 are $\Xi_c \rightarrow \Xi e^+\nu_e$ feedthrough. Details of the background estimations can be found in a previous paper [9]. The sidebands of the $p\pi$ invariant mass distribution are used to estimate the fake Λ background in this study [10]. For events in which there is a Λ candidate, we multiply the electron fake probabilities by the number of tracks not positively identified as an electron within the electron fiducial volume satisfying our kinematic criteria to estimate the fake electron background. We use the results of an earlier $\Xi_c \rightarrow \Xi e^+\nu_e$ analysis [11] and the relative efficiency for $\Xi_c \rightarrow \Xi e^+\nu_e$ to produce a Λe^+ pair passing the cuts outlined above to estimate the background from $\Xi_c \rightarrow \Xi e^+\nu_e$.

With the selection criteria described above, we find no evidence for $\Lambda e^+\nu_e$ final states in which there are additional Λ_c^+ decay products [9]. In Fig. 1, we show the $m_{\Lambda e^+}$ distribution

after Λ sideband subtraction and comparisons between the data and Monte Carlo (MC) distributions.

Calculating kinematic variables requires knowledge of the Λ_c momentum but this is unknown due to the undetectable neutrino. We estimate the direction of the Λ_c from the thrust axis of the event. The magnitude of the Λ_c momentum is then obtained by solving the equation $\vec{P}_{\Lambda_c}^2 = (\vec{P}_\Lambda + \vec{P}_e + \vec{P}_{\nu_e})^2$. After the Λ_c momentum is estimated, the four kinematic variables are obtained by working in Λ_c center-of-mass frame. The resolutions (RMS) on $t = q^2/q_{max}^2$, $\cos \Theta_\Lambda$, $\cos \Theta_W$ and χ determined by MC are 0.25, 0.25, 0.2 and 45° respectively. Due to poor resolution on χ , this angle is not used here to extract the form factor ratio.

Using t , $\cos \Theta_\Lambda$ and $\cos \Theta_W$, we perform a 3-dimensional unbinned maximum likelihood fit in a manner similar to reference [12]. This technique enables a multi-dimensional likelihood fit to be performed to variables modified by experimental acceptance and resolution, and is necessary for this analysis due to the substantial smearing of the kinematic variables. The essence of the method is to determine the probability density function by using the population of appropriately weighted Monte Carlo events in the three dimensional kinematic space. This is accomplished by generating one high statistics sample of MC events with a known value of the form factor ratio R and corresponding known values of the three kinematic variables t , $\cos \Theta_\Lambda$, and $\cos \Theta_W$ for each event. The generated events are then processed through the full detector simulation, offline analysis programs and selection criteria. Using the generated kinematic variables, the accepted Monte Carlo events are weighted by the ratio of the decay distribution for the trial values of R to that of the generated distribution. The accepted Monte Carlo events are now, therefore, distributed according to the probability density corresponding to the trial values of R . By such weighting, a likelihood may be evaluated for each data event for different values of the form factor ratio, and a fit performed. The probability for each event is determined by sampling this distribution using a search volume around each data point. The volume size is chosen so that the systematic effect from finite search volumes is small and the required number of Monte Carlo events is not prohibitively high.

The $\Lambda_c^+ \rightarrow \Lambda e^+ \nu_e$ sample has signal to background in the approximate ratio 2:1. Background is incorporated into the fitting technique by constructing the log-likelihood function $\ln \mathcal{L} = \ln \mathcal{L}_S - \ln \mathcal{L}_B$, where $\ln \mathcal{L}_S$ and $\ln \mathcal{L}_B$ are the log-likelihood calculated for events in the signal region and for the background events respectively and both likelihoods are evaluated for the same shape (method A). In this way the background contribution to the log-likelihood function is subtracted directly, however this method does not include fluctuations of the background in the statistical error on the fit parameters and therefore will underestimate the statistical error. To account for background fluctuations in the fit and to investigate the systematic error associated with the method of background incorporation into the fit we construct the function $\ln \mathcal{L} = \sum_{i=1}^N \ln(P_S \Gamma_S + P_B \Gamma_B)$, where N is the number of events in the signal region, P_S and P_B are the probabilities that events in this region are signal and background respectively, and Γ_B is a model of the background (method B). With small background samples it is difficult to evaluate the background shape Γ_B . In this preliminary analysis we use method A to determine the central value and method B to determine the statistical error on the central value. We take the difference in the central value found by the two methods as the systematic error due to the method of background incorporation.

The 1101 events in the signal region are fit to the expression for the decay rate, Γ_S , using 60,000 accepted MC events. We find $R = -0.33 \pm 0.16$ where the errors are statistical. Fig. 2 and Fig. 3 show the projections of the t , $\cos \Theta_\Lambda$ and $\cos \Theta_W$ distributions for the data and for the fit. The confidence level of the fit is determined by the K nearest neighbours method [13] and by comparing the likelihood of the fit with the distribution of likelihoods obtained by fitting many MC samples of the same number of events as the data sample. Both methods give a consistent result. The hypothesis that the signal is described by the KK model with $R = -0.33$ has a confidence level of 23%.

The systematic error on R arises from Monte Carlo statistics, volume size used in the likelihood fit, uncertainties in the background normalization and the method of background incorporation. The error due to Monte Carlo sample size is estimated by dividing the Monte Carlo into six equal samples and repeating the fit. The systematic error due to the size of the search volume is determined by varying the volume size and repeating the fit. The largest difference obtained is taken as the systematic error from this source. The systematic error associated with the background normalization is determined by varying the estimated number of the background events in the signal region by one standard deviation. The largest systematic error is due to the manner of background incorporation. It is estimated from the difference between the central values found by method A and method B. This error is taken to be symmetric in the final result. Combining all of the above errors in quadrature we find:

$$R = -0.33 \pm 0.16 \pm 0.15$$

In conclusion, using a 3-dimensional maximum likelihood fit the angular distributions of $\Lambda_c^+ \rightarrow \Lambda e^+ \nu_e$ have been studied. The form factor ratio, $R = f_2/f_1$, is extracted to be $-0.33 \pm 0.16 \pm 0.15$ with 23% confidence level.

We gratefully acknowledge the effort of the CESR staff in providing us with excellent luminosity and running conditions. This work was supported by the National Science Foundation, the U.S. Dept. of Energy, the Heisenberg Foundation, the SSC Fellowship program of TNRLC, Natural Sciences and Engineering Research Council of Canada, and the A.P. Sloan Foundation.

REFERENCES

- [1] Particle Data Group, Phys. Rev. Lett. **45** 1 (1992).
- [2] N. Isgur and M.B. Wise, Phys. Lett. **B232** 113 (1989); N. Isgur and M.B. Wise, Phys. Lett. **B237** 527 (1990); E. Eichten and B. Hill, Phys. Lett. **B234** 511 (1990); H. Georgi, Phys. Lett. **B240** 447 (1990).
- [3] T. Mannel, W. Roberts and Z. Ryzak, Nucl. Phys. **B355** 38 (1991).
- [4] T. Mannel, W. Roberts and Z. Ryzak, Phys. Lett. **B255** 593 (1991); F. Hussain, J.G. Körner, M. Krämer and G. Thompson; Z. Phys. **C51** 321 (1991).
- [5] J.G. Körner and M. Krämer, Phys. Lett. **B275** 495 (1992).
- [6] H. Georgi, B. Grinstein and M.B. Wise, Phys. Lett. **B252** 456 (1990); N. Isgur and M.B. Wise, Nucl. Phys. **B348** 276 (1991); H. Georgi, Nucl. Phys. **B348** 293 (1991).
- [7] Y. Kubota *et al.*, Nucl. Instr. and Meth. **A320** 255 (1992).
- [8] Throughout this paper charge conjugate modes are implicitly included.
- [9] T. Bergfeld *et al.* (CLEO), Phys. Lett. **B323** 219 (1994).
- [10] In ref [9] the fake Λ background was allowed for by fitting the $p\pi$ invariant mass. The Λ sideband method used in this work gives a consistent estimate of the fake Λ background.
- [11] J. Alexander *et al.* (CLEO), Contributed paper to this conference, GLS0245 and submitted to Phys. Rev. Lett. (1994).
- [12] D.M.Schmidt, R.M.Morrison and M.S.Witherell, Nucl. Instr. and Meth. **A328** 547 (1993).
- [13] J.H. Friedman, CERN 74-23 271(1974).

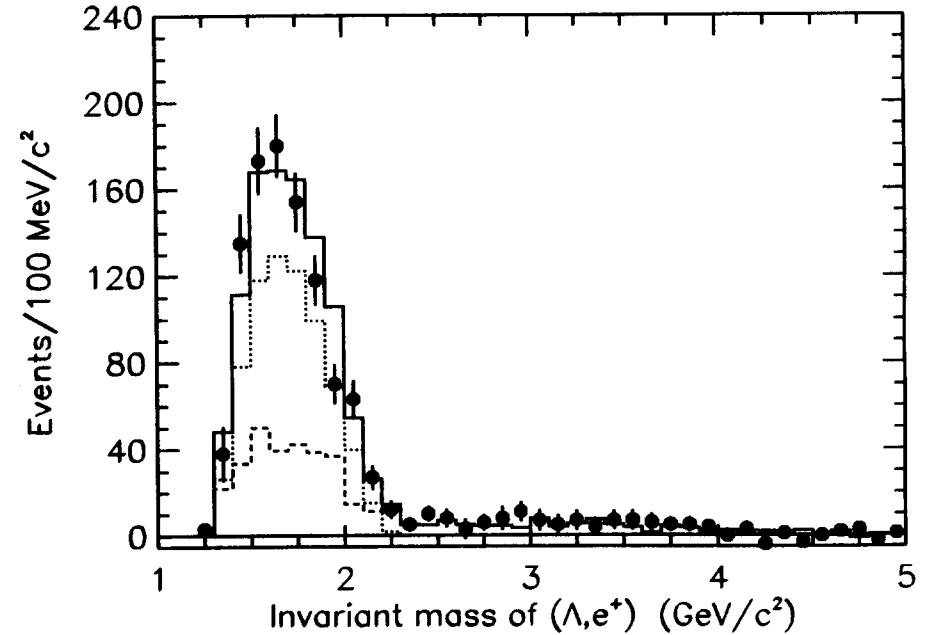


FIG. 1. Invariant Λe^+ mass for right sign combinations. The points with error bars are data after subtraction of the contribution of fake lambdas estimated using the $p\pi$ invariant mass sidebands. The dashed line shows the sum of the backgrounds described in the text. The dotted line shows the Monte Carlo prediction for $\Lambda_c^+ \rightarrow \Lambda e^+ \nu_l$ normalized to the data after subtraction of the backgrounds. The solid line shows the sum of the Monte Carlo prediction and the backgrounds.

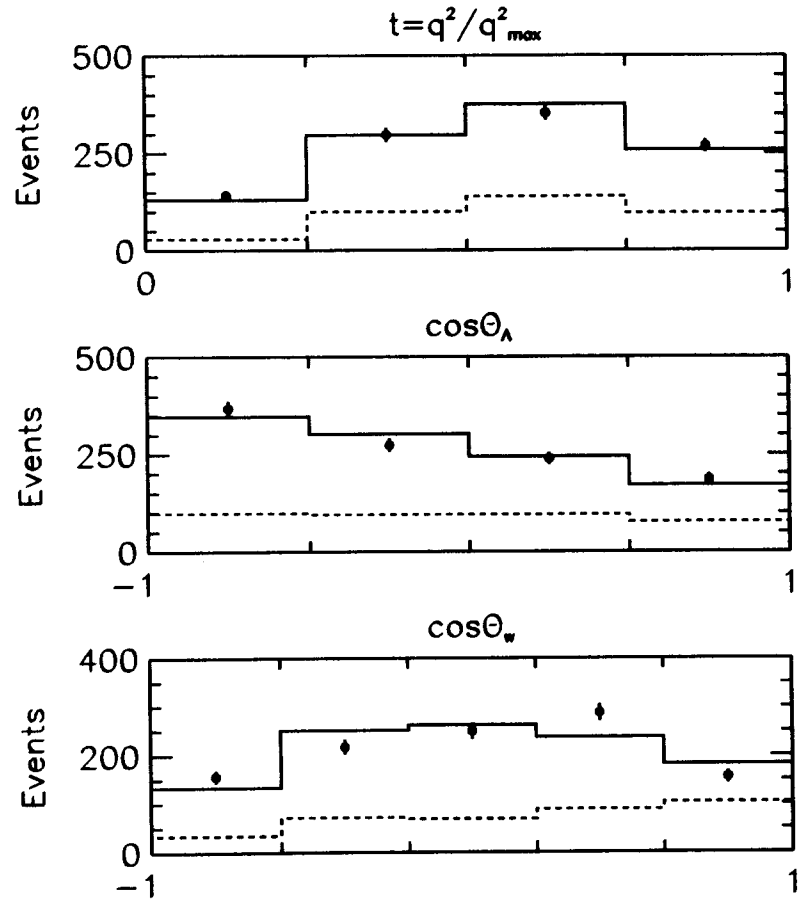


FIG. 2. Projections of the data (points with error bars) and the fit (solid histogram) for t , $\cos\theta_A$ and $\cos\theta_W$. The dashed lines show the background distributions.

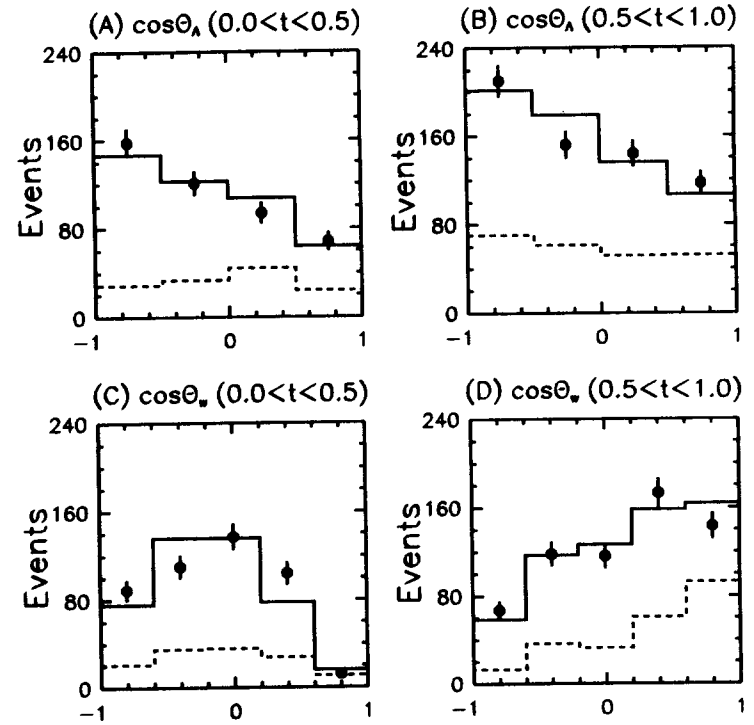


FIG. 3. Projections of the data (points with error bars) and the fit (solid histogram) onto $\cos\theta_A$ and $\cos\theta_W$ for different t regions. (A) and (C) are for $0.0 < t < 0.5$ and (B) and (D) are for $0.5 < t < 1.0$. The dashed lines show the background distributions.

